WEAR PROPERTIES OF ALUMINUM MATRIX COMPOSITES REINFORCED BY GRAPHENE ENCAPSULATED SiC NANOPARTICLES

S. GUO[a], J. B. GAO[b], X. M. DU[a], G. S. FANG[a], H. T. QI[a], N. LI[a], G. ZHANG[a*]
[a] School of Materials Science and Engineering, Shenyang Ligong University, Shenyang 110159, China.
[b] Centre of Excellence for Advanced Materials, Dongguan 523808, China.

Graphene encapsulated SiC nanoparticles reinforced aluminum matrix composites were prepared by high energy ball-milling and hot-press sintering methods. The effect of graphene content on microstructure and wear properties of composites was investigated. The results show that the graphene sheets successfully encapsulates SiC nanoparticles to form a composite reinforcement phase under the condition of the graphene content of 1 wt.%. SiC nanoparticles encapsulated with graphene predominantly are homogeneously distributed on the grain boundaries of Al matrix. The interface between graphene and Al matrix is sharpand no Al-C compound is formed on the interface. The increase of the reinforcement phase reduces the wear performance of the composite material. The main wear mechanisms of aluminum-based composite materials are the combination of delamination wear and abrasive wear. As the graphene content increases, the wear mechanism changes from abrasive wear to delamination wear.

1. Introduction

Aluminum matrix composites(AMCs), one of the most commonly used in metal matrix composites(MMCs), have been widely used in the aerospace, military, automotive and other industrial fields due to excellent mechanical and tribological properties, easy formability and low density[1-4]. SiC particles were once considered to be one of the ideal materials for the production of aluminum matrix composites due to their low cost and high reinforcement efficiency[5].There had been many studies on the properties of SiC particles reinforced aluminum matrix composites that are gaining importance because of their low cost with advantages like isotropic properties and the possibility of secondary processing facilitating fabrication of secondary components [6-8].However, there are also some problems that are not resolved, restricting the application of composite materials, such as poor ductility and low fatigue resistance.

In recent years, graphene reinforced aluminum metal matrix composites have been studied due to the extraordinary properties of graphene: excellent electric properties [9], high thermal conductivity [10], high Young's modulus [11] and high tensile stress [12].Wang et al [13] reported that the tensile strength of Al composite reinforced with only 0.3 wt-% graphene nanosheets by powder metallurgy is 249 MPa. It was 62% enhancement over the unreinforced Al matrix. Li et al.[14] reported that the Al composite reinforced with only 0.3 wt.% of graphene oxide shows an 18 and 17% increase in elastic modulus and hardness, respectively, over unreinforced Al. Yan Shao-jiu et al.[15] reported that the tested tensile strength and yield strength of 0.3 wt%

---

* Corresponding author: gangzhang_imr@163.com

graphene-reinforced Al matrix composites fabricated by powder metallurgy, compared to the pristine Al alloy, show an increase of 25 and 58%, respectively. Nowadays, SiC and graphene reinforced hybrid composites are rarely studied to create the synergic effect due to the superior solid lubricant properties of graphene and the great wear resistance, hardness, and compressive strength of SiC. Boostani et al. presented the enhancement of tensile properties of A356aluminum composites reinforced with graphene encapsulated SiC particles using ultrasonic vibration casting method. Compared to A356 aluminum alloy, yield strength (+ 45%) and tensile ductility (+84%) of composites increased with binary SiC- graphene reinforcement [16]. Ghazaly et al. studied the graphene-coated SiC nanoparticles for tribological applications of 2124 aluminum alloy. They reported the better densities, higher hardness, greater tensile properties using binary SiC- graphene materials when compared to Al2124 alloy [17].Although some valuable researches have been concentrated on the effect of pure SiC and graphene reinforced aluminum composites, there are rare studies on the SiC and graphene reinforced hybrid composites.

In the present work, SiC nanoparticles encapsulated by graphene for various ratios are reinforced to the Al7075 matrix by powder metallurgy method. This study aims to investigate and compare the effect of synergistic graphene-encapsulated SiC addition on the microstructure and tribological properties of aluminum hybrid composites.

2. Experimental procedures

2.1. Materials

Aluminum alloy 7075 (10–20μm particle size) and SiC nanoparticles (99%purity and <100 nm particle size) were provided from Beijing Hongyu Materials Co., Ltd. and Shanghai Yunfu Nanotechnology Co., Ltd., respectively, commercially. SiC and graphene nanosheets were used as reinforcement elements to prepare Al-SiC-graphene hybrid composites by powder metallurgy method. Graphene nanosheets (a diameter of 5-10 μm and a thickness of 3-10 nm) were purchased from Nanjing XFNANO material Technology Co., Ltd. (China).

2.2. Methods

Al7075 hybrid metal matrix composites (Al-graphene-SiCp) were fabricated by powder metallurgy. In this method, graphene nanosheet and SiC powders with the weight ratio of 2:1, 1:1 and 1:2were first milled without aluminium powder to obtain graphene-encapsulated SiC composite powders in an planetary ball mill without interruption under high purity(99.999%) argon gas, in which the rotation rate is 300 rpm and the zirconia balls to powder weight ratio is 15:1 under a total milling time of 3 h. Subsequently, the milling was continued for 3 h by add in galuminium powder to the composite powders, containing graphene and SiC, by setting the aluminium weight equal to 99.25, 99, 98.5 wt.% of the total powders, to obtain Al-SiC-graphene hybrid composites that the amount of graphene nanosheet is 0.25, 0.5, 1.0wt.% and 0.5 wt.% for SiC nanoparticles, respectively.

The composite powders were consolidated under vacuum in hot-pressed furnace at 610°C for 3 hours under a pressure of 30 MPa using graphite paper as lubricants between the punch and die walls. The composite samples were treated by solid solution treatment at 470 °C for 2 h, and quenched with cold water. Then artificial aging was carried out at 140 °C for 16 h.

2.3. Characterizations

Reciprocating friction and wear tester (MDW-02,Jinan,China) was used for dry sliding wear test. All samples are polished before wear testing to ensure that the surface of the sample has the same roughness. The dry wear tests were carried out at room temperature using the load of 10 N. Balls with diameter 6.35mm and made of GCr15 bearing steel (HRC63 ±3) were used for the wear tests. These wear tests were carried out at a frequency of 1 Hz for 20 minutes. The surface morphology of the composites was observed by TESCAN scanning electron microscope ((SEM)) equipped with EDS. In addition, in order to investigate the formation of graphene sheets in the matrix and around the SiC particles in the composite, transmission electron microscope(TEM) was employed using a JEM-2100F at an accelerating voltage of200 kV. The worn surface was observed and analyzed by scanning electron microscope (Hitachi Smer 3400, Japan).

3. Results and discussion

Fig. 1(a)-(f) illustrates the SEM and EDS mapping images of the Al-0.25graphene-0.5SiC, Al-0.5graphene-0.5SiC, and Al-1.0graphene-0.5SiC composites. In Fig. 1(a), a small amount of SiC nanoparticles can be observed at the grain boundary, but graphene is not observed. It is likely because that the content of graphene is low and it is difficult to identify duo to a large number of wrinkles on the surface of graphene sheets. In addition, no agglomeration of reinforced particles was found. An enlarged view of the corresponding region of Fig. 1(a) is shown in Fig. 1(b). Further, the inset shows the EDS results which was done on same SEM selected area. The analysis shows the presence of all major alloying elements such as Zn and Mg of the Al 7075. The most important inference from the analysis is the presence of graphene and SiC at the grain boundary.

The surface morphology of Al-0.5graphene-0.5SiC is shown in Fig. 1(c) and (d). It can be found that there is a black aggregate at the grain boundary. It can be found that the content of C element is very high, and the content of Si has not been detected from EDS analysis. It is indicated that the black aggregate is graphene sheets. Fig. 1(d) is an enlarged view of the corresponding area of Fig. 1(c), it can be seen from Fig.1 (d) that the graphene surface maintains the original fold, and no new compound is produced at the junction with the matrix. In addition, the size of graphene sheets observed is about 3μm.

Fig. 1(e) and Fig. 1(f) show the surface morphology of Al-1.0graphene-0.5SiC. Graphene sheets and SiC nanoparticles can be obviously observed, and these reinforced phases are distributed at the grain boundary. It is worth noting that a larger graphene sheets were found in Al-1.0graphene-0.5SiC composite (Fig. 1(e)).It can be seen from the magnification of the graphene region in Fig. 1(e), as shown in Fig. 1(f), it can be found that there are a large number of folds on the graphene sheets. Moreover, graphene sheets are closely connected with SiC nanoparticles. The part of SiC nanoparticles is wrapped in graphene sheets. The illustration in Fig. 1(f) is the EDS result of the graphene region, where the red dots and blue dots represent the C and Si elements, respectively. It can be found that there are the numerous C elements and a small amount of Si elements that are distributed among C elements. This proves that graphene sheets successfully encapsulates SiC nanoparticles to form a composite reinforcement phase.

(a)   *(b)*   *(c)*

(c)   *(d)*   *(f)*
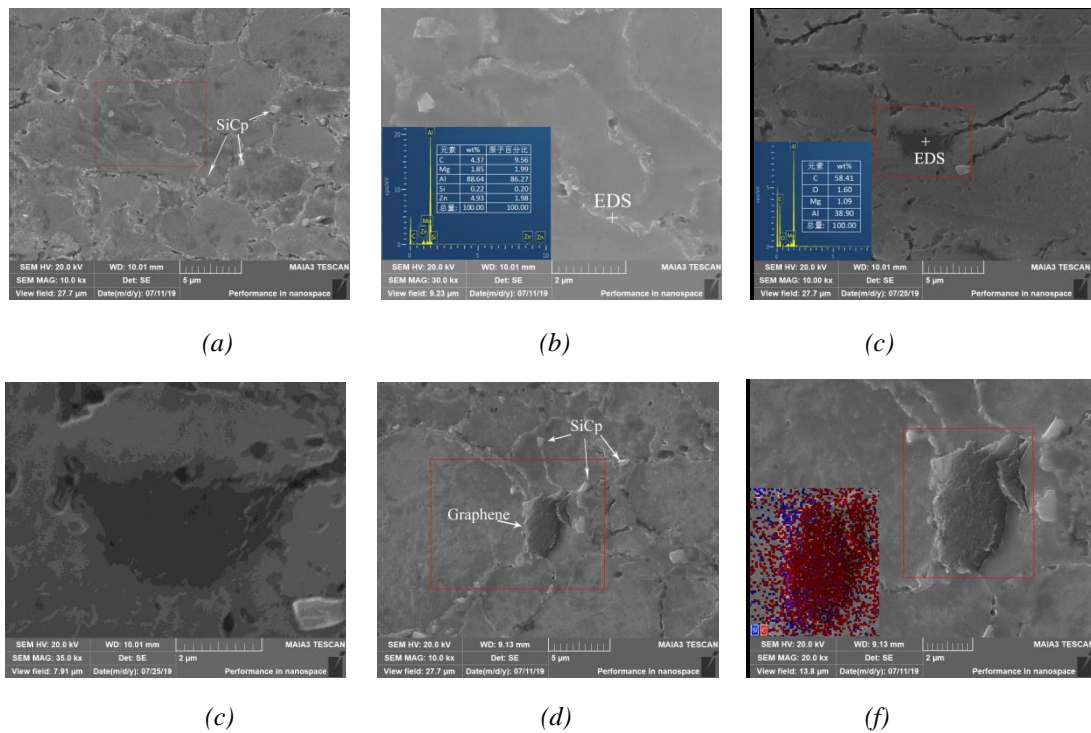
Fig. 1 SEM morphology of composites, (a) Al-0.25graphene-0.5SiC,(b) Local magnification in(a), (c) Al-0.5graphene-0.5SiC, (d) Local magnification in (c), (e)Al-1.0graphene-0.5SiC, (f) Local magnification in (e).

TEM was used to observe and identify graphene sheets and SiC nanoparticles in the Al matrix composites. The TEM bright field image its distribution of elements mapping of C and Si forAl-1.0graphene-0.5SiC composite are shown in Fig.2. As can be seen from the Fig. 2(a), there is an obvious sheet structure with the size of several micrometers. Fig. 2 (b) and 2(c) show the element distribution of C and Si in the surface of sheet structure. It can be found that there are blue spots of Si in the area covered by the red spots of C, indicating that the SiC nanoparticles are coated with graphene.

(a)   *(b)*   *(c)*
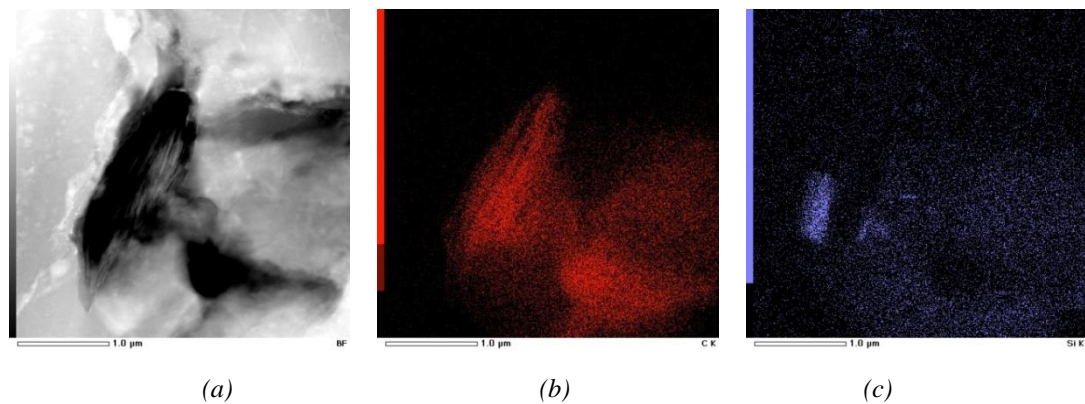
Fig. 2.(a) TEM bright field image of Al-1.0graphene-0.5SiC composite, the distribution of elements mapping of (b) C, (c) Si.

TEM bright field images of Al-1.0graphene-0.5SiCare shown in Fig. 3. As shown in Fig. 3(a), the lighter part of the picture is graphene, and there are many folds on its surface, which is the same as that reported in the literatures [18-20].Fig. 3(b) is an magnification of the corresponding portion in Fig. 3(a). The interface between graphene and Al matrix can be clearly observed in Fig. 3(b). Al_4C_3 showed a black lath shape, slightly loosely multilayered, with a width of 5-10nm and a length of 20-50nm, which existed near the bonding interface were clearly observed using TEM carbon in Al2024 composites reinforced by nanotube [21]. Zhang et al. [22]reported that the morphology of Al_4C_3 observed under TEM for Al5083 composites reinforced by graphene was the same as that in literature [21]. No Al_4C_3 was found in Fig. 3(b), indicating that the interface between graphene and Al matrix is mechanically bonded and the bonding is very close. It is worth noting that the stacking marks of SiC nanoparticles with edges and corners can be vaguely observed on the graphene layer. This proves that SiC nanoparticles are successfully coated by graphene to form a composite reinforcement phase.

Fig. 3(c) shows a cross-sectional view of the graphene-coated SiC nanoparticles in Al-1.0graphene-0.5SiC. The black part is the SiC nanoparticle, and the lighter color partaround the black part is graphene. It can be clearly observed that the interface between graphene and SiC nanoparticles is sharp. No compound is formed. Fig. 3(d) is a magnification of the corresponding partin Fig. 3(c)in which the interface between reinforced phases (SiC nanoparticles and graphene) and aluminum matrix can be clearly observed. The loose and multi-layer aluminum carbide was formed on the interface between SiC and aluminum matrix[23]. The formation of Al4C3 affects the strengthening effect of the reinforcement relative to the matrix and adversely affects the mechanical properties of aluminum matrix composites. The reaction between aluminum alloy matrix and SiC nanoparticles can be avoided by the presence of graphene. In Fig. 3(d), the different interface characteristics of SiC nanoparticles in contact with graphene and aluminum alloy matrix can be clearly observed. Al_4C_3 is not found in the present work.

(a)

(b)

(c)

(d)
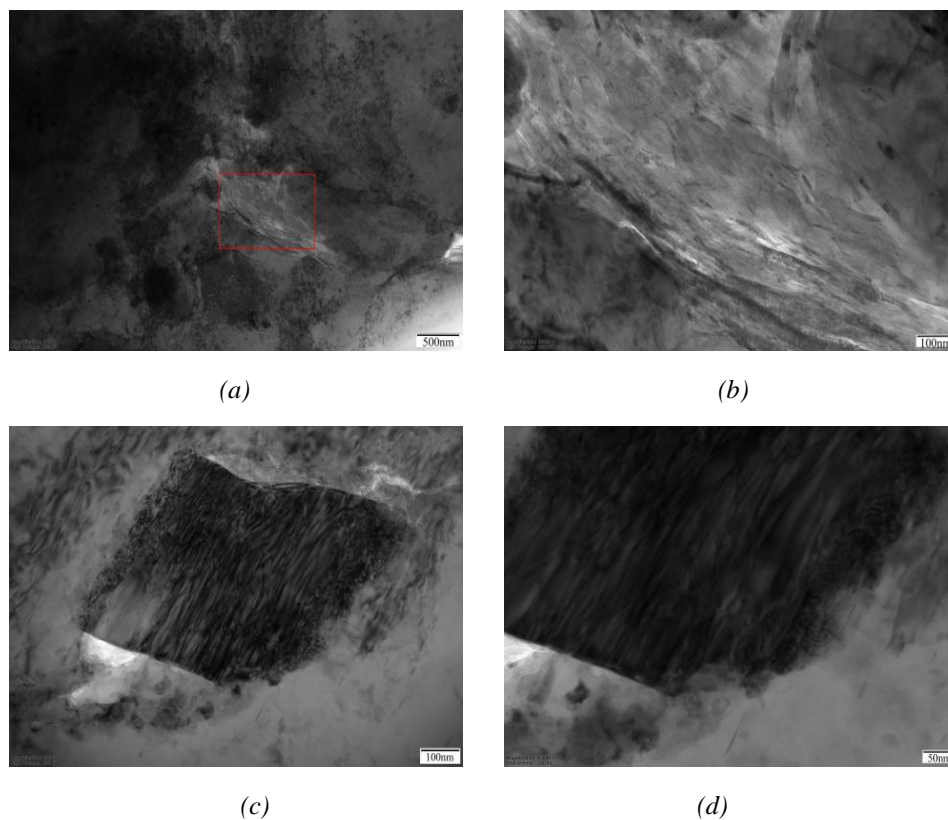
Fig. 3 TEM bright field image of Al-1.0graphene-0.5SiC composite,(a) microscopic morphology of graphene,

(b) the magnification of corresponding region in (a), (c) microscopic morphology of SiC nanoparticles (d)

the magnification of corresponding region in (c).

Fig. 4 shows the wear cross sections of the composite material samples. The specific wear cross-sectional area are also marked in the Figures. It can be found that as the mass fraction of the graphene-SiC nanoparticle reinforced phase increases, the worn cross-sectional area becomes larger. This indicates that the increase of the reinforcement phase reduces the wear performance of the composite material. The main reason is that the addition of the reinforced phase leads to a decrease in the density of the composite material. When subjected to friction and wear, the composite material is more likely to be peeled off due to the existence of more porous holes equivalent to more micro-cracks hidden in the material.

(a) *(b)*

(c)
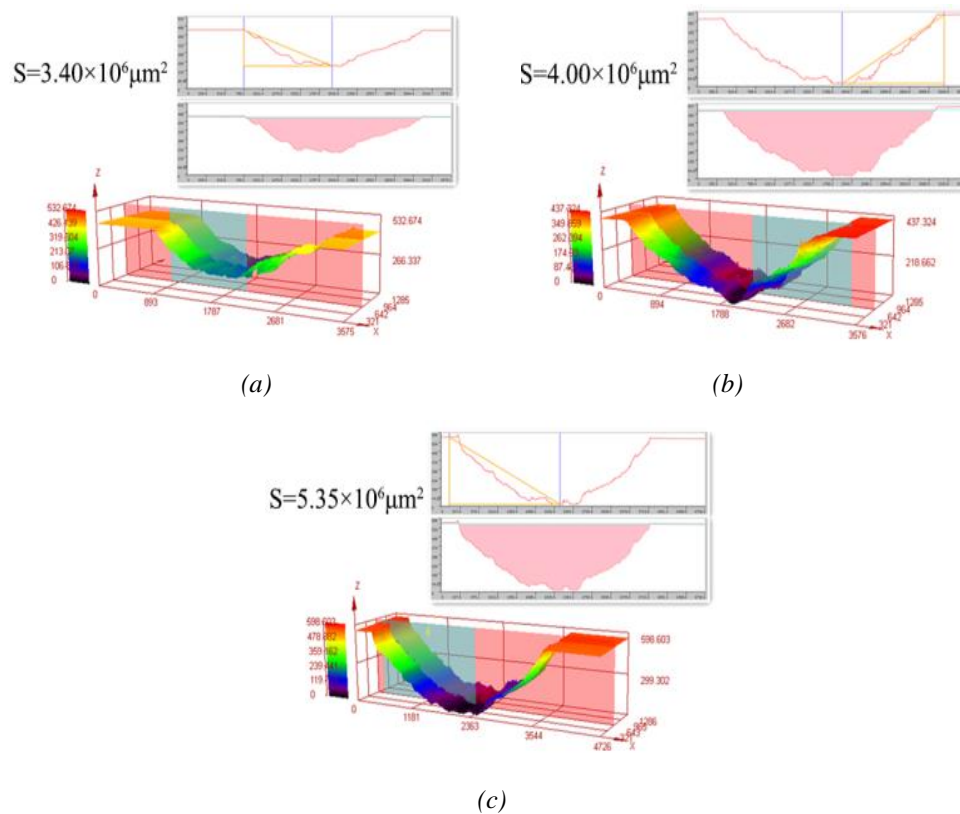
Fig. 4 Wear cross section of composites, (a) Al-0.25 graphene-0.5SiC, (b) Al-0.5 graphene-0.5SiC,
(c) Al-1.0 graphene-0.5SiC.

The tribological properties of the composites are shown in Fig. 5. Fig. 5a is a graph of the width and depth of the wear section. It can be seen more intuitively from the Fig. 5(a) that with the increase of the composite reinforced phase (graphene-coated SiC nanoparticles), the width of the wear cross section is first flat and then increases rapidly, while the depth continues to increase. This is consistent with the results in Fig. 4. Fig. 5(b) shows that the specific wear rate of the composite varies with the content of the reinforced phase. It can be found that the content of the reinforced phase is the main reason that affects the specific wear rate. The specific wear rate increases significantly with the increase of the content of the reinforcements. It is indicated that the wear resistance of the composites decreases with the increase of the content of the reinforcements. The average friction coefficient of the composite materials increase is shown in Fig. 5(c). It can be seen that the average friction coefficient first decreases and then increases as the content of the

reinforced phase increases. This is due to the lubricating effect of graphene in composite materials [24]. The graphene will form a dense self-lubricating layer on the worn surface during the wear process[25], thereby reducing the friction coefficient of the composite material. However, the addition of graphene will also increase the porosity and cause pore defects in the composite material. This causes that the friction coefficient fluctuates greatly with the sliding distance. At the same time, the porosity caused by the addition of graphene is also the main reason for the change in the width, depth and specific wear rate of the wear section.

(a)

(b)

(c)
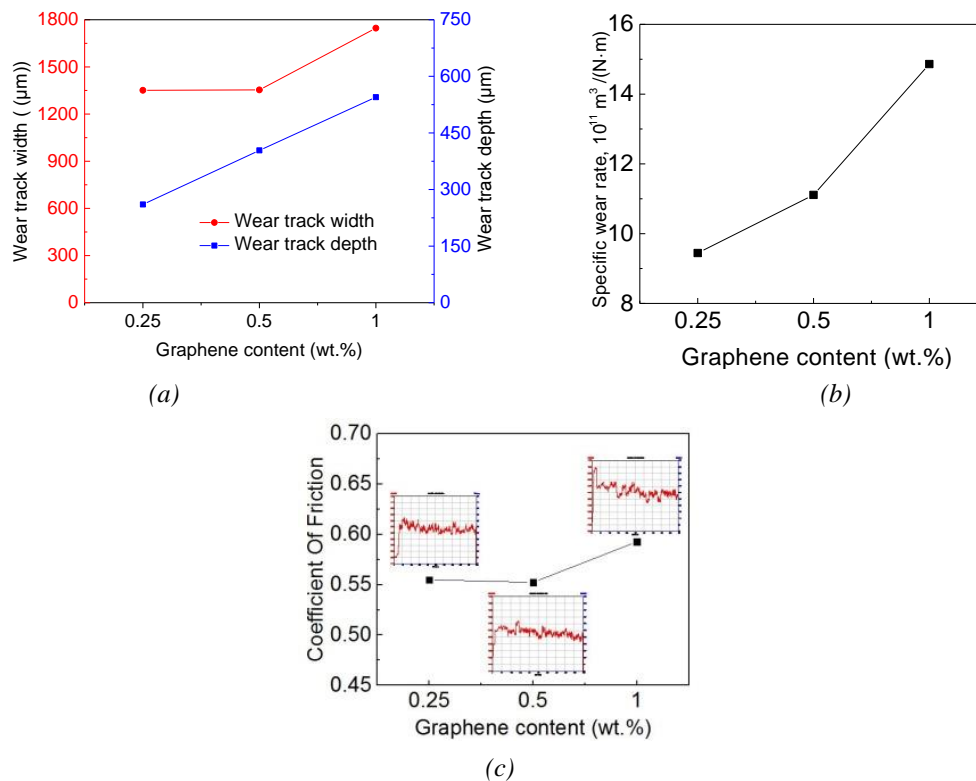
Fig. 5 Tribological properties of composites, (a) the width and depth of the wear section, (b) the specific wear rate of the composite, (c) The average friction coefficient of the composite.

Fig. 6 shows the SEM morphology of the worn surface of the composite material. It can be found that the local area of the wear surface of the composite material sample shows the material flow along the sliding direction and the peeling direction, which indicates the existence of a delamination wear mechanism[26]. As the content of the reinforced phases in the composite material increases, the material flow traces decrease and the number of wear pits increases. The wear pits are caused by the material being peeled off during the delamination wear process. This indicates an increase in delamination wear. In addition, the furrows left by abrasive wear can be observed in Fig. 6(a), (b), and (c). In contrast, the wear surface morphology of Al-0.25 graphene-0.5SiC (Fig. 6(a)) is shallower. For Al-0.5 graphene-0.5SiC (Fig. 6(b))) and Al-1.0 graphene-0.5SiC (Fig. 6(c)), the furrows are deeper in the worn surface morphology. As the delamination wear intensified, the part of the furrow traces were destroyed. It is impossible to compare the changes in the furrows in terms of furrow quantity. It can be considered that the main

wear mechanisms of aluminum-based composite materials are the combination of delamination wear and abrasive wear. With the increase of the content of the reinforced phases in composites, the delamination wear and abrasive wear of the composites both show an increasing trend.

(a)

(b)

(c)
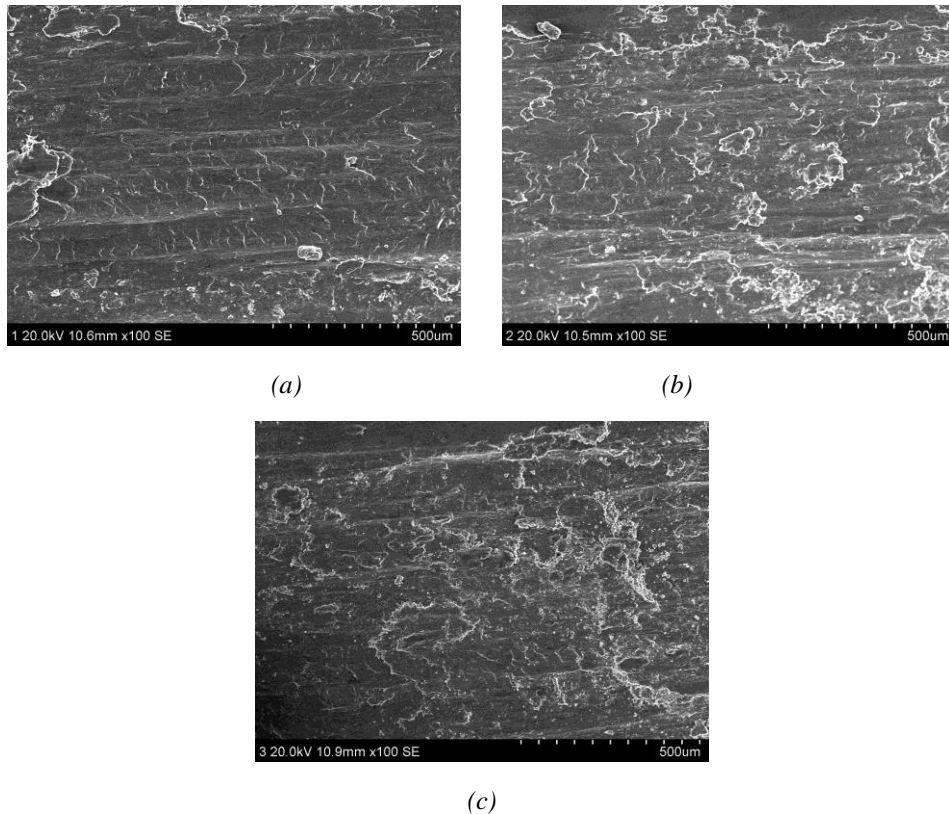
Fig. 6 Wear surface morphology of composites, (a) Al-0.25 graphene-0.5SiC,
(b) Al-0.5 graphene-0.5SiC, (c) Al-1.0 graphene-0.5SiC.

The shape and size of abrasive debris can provide clues to existing wear mechanisms and provide information about the state of wear. Fig. 7 shows the SEM micrographs of the wear debris of three composites. According to the shape and size of the abrasive debris, it can be divided into three types: (1) Flake abrasive debris. This type of wear debris is the most common form, ranging in size from 100μm to 300μm. These sheets with a thickness of 10μm to 30μm can be observed in Fig. 7(b) and (c). The debris is caused by the adhesion and delamination of the friction pairs in the sliding direction. (2) Fine debris. Contrary to larger flaky abrasive debris, the fine debris has a size of about 1μm to 50 μm and is generally granular. The generation of fine abrasive debris is attributed to the abrasive micro-cutting effect. In general, the smaller the size of the abrasive debris, the better the wear resistance of the material.(3) Corrugated debris. It can be observed that the amount of such debris is very small. There are many distinct layers on the surface of the debris. This is mainly due to the combined action of shear force and constant friction in the sliding direction [27,28]. By comparing Fig.7(a), (b), and (c), it can be found that the number of fine abrasive debris decreases while flake abrasive debris increases as the content of the reinforced phases in the aluminum-based composite increases, indicating a decrease in wear resistance.

(a)

(b)

(c)
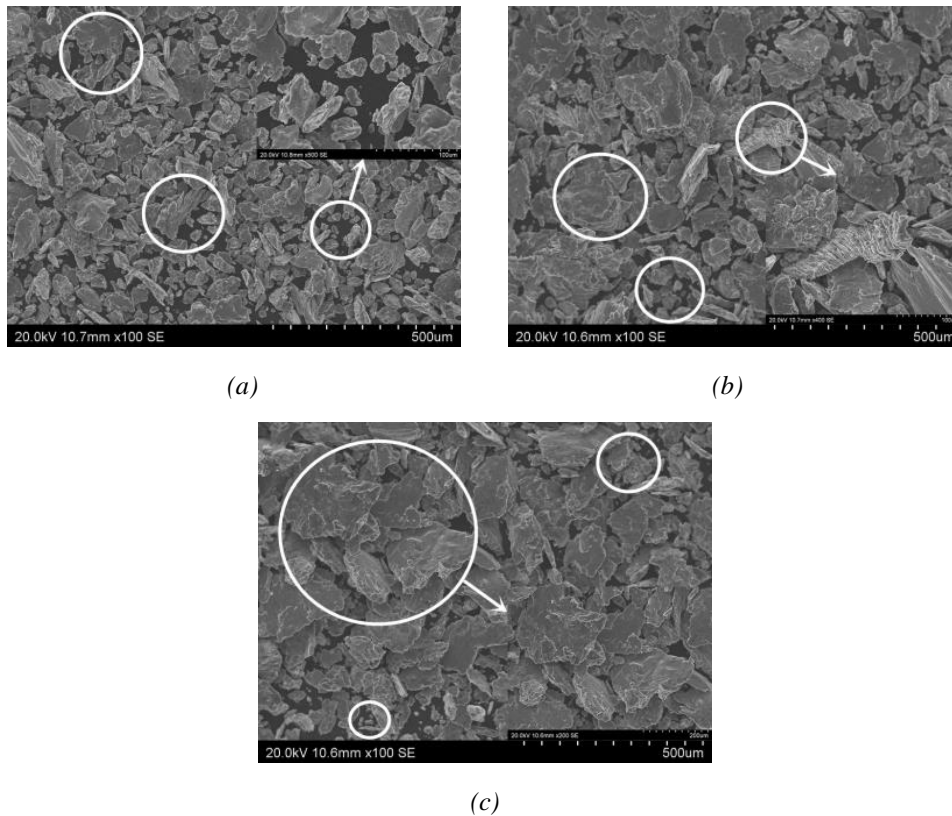
Fig. 7 Micrographs of wear debris of composites, (a) Al-0.25 graphene-0.5SiC,
(b) Al-0.5 graphene-0.5SiC, (c) Al-1.0 graphene-0.5SiC.

4. Conclusion

In this study, Al7075 composites reinforced by SiC nanoparticles coated graphene were fabricated using by high energy ball-milling and hot-press sintering methods. SEM and TEM analysis show that the graphene sheets successfully encapsulates SiC nanoparticles to form a composite reinforcement phase under the condition of the graphene content of 1 wt.%. SiC nanoparticles encapsulated with graphene predominantly are homogeneously distributed on the grain boundaries of Al matrix.

The interface between graphene and Al matrix is sharp and no Al-C compound is formed on the interface. The increase of the reinforcement phase reduces the wear performance of the composite material, in which the addition of the composite reinforcing phase lead into the porosity, resulting in a decrease in the wear resistance of the composite materials. The main wear mechanisms of aluminum-based composite materials are the combination of delamination wear and abrasive wear. As the graphene content increases, graphene can accumulate at the wear scars and form a dense lubrication layer to prevent further aggravation of wear. And then the wear mechanism changes from abrasive wear to delamination wear.

258

References

[1] S. N. Alam, L. Kumar, Mater. Sci. Eng. A**667**, 16 (2016).

[2] N. Panwara, A. Chauhan, Mater. Today: Proc.**5**, 5933(2018).

[3] J. Liu, U. Khan, J. Coleman, B. Fernandez, P. Rodriguez, S. Naher, D. Brabazon, Materials & design**94**, 87 (2016).

[4] M. O. Bodunrin, K. K. Alaneme, L. H. Chown, J. Mater. Res. Tech. **4** (4), 434 (2015).

[5] Z. Wang, C. Li, H. Wang, X. Zhu, M. Wu, J. Li, Q. Jiang, J. Mater. Sci. Technol. **32**, 1008 (2016).

[6] Y. Sumankant, C. S. Jawalkar, A. S. Verma, N. M. Suri, Mater. Today: Proc. **4**, 2927 (2017).

[7] A. P. Reddy, P. V. Krishna, R. N. Rao, N. V. Murthy, Mater. Today: Proc. **4**, 3959 (2017).

[8] T. P. D. Rajan, R. M. Pillai, B. C. Pai, K. G. Satya Narayana, P. K. Rohatgi, Compos. Sci. Technol. **67**, 3369 (2007).

[9] K. S. Novoselov, A. K. Geim, S. V. Morozov, D. Jiang, Y. Zhang, S. V. Dubonos, I. V. Grigorieva, A. A. Firsov. Science **306**, 666 (2004).

[10] A. A. Balandin, S. Ghosh, W. Bao, I. Calizo, D. Teweldebrhan, F. Miao, C. N. Lau, Nano Lett. **8**, 902 (2008).

[11] C. Lee, X. Wei, J. W. Kysar, J. Hone, Science **321**, 385 (2008).

[12] C. Lee, X. Wei, Q. Li, R. Carpick, J.W. Kysar, J. Hone, Phys. Status Solid (B) **246**, 2562 (2009).

[13] J. Wang, Z. Li, G. Fan, H. Pan, Z. Chen, and D. Zhang, Scripta Materialia **66**, 594 (2012).

[14] Z. Li, G. Fan, Z. Tan, Q. Guo, D. Xiong, Y. Su, Z. Q. Li, D. Zhang, Nanotechnology **25**, 325601 (2014).

[15] S. J. Yan, Y. Cheng, H. Q. Hu, C. J. Zhou, L. D. Bo, D. S. Long, J. Mater. Eng. **4**, 1 (2014).

[16] A. F. Boostani, S. Tahamtan, Z. Y. Jiang, D. Wei, S. Yazdani, Compos Part A-Appl S **68**, 155 (2015).

[17] A. E. Ghazaly, M. Shokeir , S. N. E. Moghazi, A. Fathy, Nanocomposites mechanical and tribological properties using graphene-coated-SiC nanoparticles (GCSiCNP) for light weight applications. Part of the Minerals, Metals & Materials Series Book Series (MMMS), In: Proceedings of the 3rd Pan American Materials Congress, 2017, 403-15.

[18] X. Gao, H. Yue, E. Guo, H. Zhang, X. Y. Lin, Materials & design **94**, 54 (2016).

[19] H. Yue, L. Yao, X. Gao, S. Zhang, B. Wang, J. Alloy Compd. **691**, 755 (2017).

[20] M. Rashad, F. Pan, Z. Yu, A. Muhammad, L. Han, R. Pan, Progress in Natural Science: Materials International **25**(5), 460 (2015).

[21] S. E. Shin, Y. J. Ko, D. H. Bae, Composites Part B: Engineering **106**, 66 (2016).

[22] H. Zhang, C. Xu, W. Xiao, K. Ameyama, C. Ma, Mater. Sci. Eng. A**658**, 8 (2016).

[23] A. F. Boostani, R. T. Mousavian, S. Tahamtan, S. Yazdani, R. Azari Khosroshahi, D. Wei,

J. Z. Xu, D. Gong, X. M. Zhang, Z. Y. Jiang, Mater. Sci. Eng. A**648**, 92 (2015).

[24] D. Berman, A. Erdemir, A. V. Sumant, Materials Today **17**(1), 31 (2014).

[25] W. Zhai, X. Shi, M. Wang, Z. Xu, Y. Jie, S. Song, Y. Wang, Wear **310**(1-2), 33 (2014).

[26] M. R. Akbarpour, M. Najafi, S. Alipour, H. S. Kim, Materials Today Communications **18**, 25 (2019).

[27] J. Zhang, S. Yang, Z. Chen, Wu Hui, J. Zhao, Z. Jiang, Composites Part B: Engineering **162**, 445 (2019).

[28] S. Kumar, R. S. Panwar, O. P. Pandey, Ceramics International **39**(6), 6333 (2013).